Cascieri, M. A., Chicchi, G. G., Applebaum, J., Hayes, N. S., Green, B. G., & Bayne, M. L. (1989) *J. Biol. Chem. 264*, 2199–2202.
Czech, M. P. (1989) *Cell 59*, 235–238.
DeVroede, M. A., Rechler, M. M., Nissley, S. P., Joshi, S., Thompson Burke, G., & Ktsoyannis, P. G. (1985) *Proc. Natl. Acad. Sci. U.S.A. 82*, 3010–3014.
Dodson, E. J., Dodson, G. G., Hodgdin, D. C., & Reynolds, C. D. (1974) *Can. J. Biochem. Cell Biochem. 57*, 469–479.
Duckworth, W. C. (1988) *Endocrine Rev. 9*, 210–233.
Duckworth, W. C., & Kitabchi, A. E. (1981) *Endocrine Rev. 9*, 319–345.
Duckworth, W. C., Hamel, F. G., Peavy, D. E., Liepnieks, J. J., Ryan, M. P., Hermodson, M. A., & Frank, B. H. (1988) *J. Biol. Chem. 263*, 1826–1833.
Duckworth, W. C., Garcia, J. V., Liepniecks, J. J., Hamel, F. G., Hermodson, M. A., Frank, B. H., & Rosner, M. R. (1989) *Biochemistry 28*, 2471–2477.
Ellis, L., Clauser, E., Morgan, D. O., Edery, M., Roth, R. A., & Rutter, W. J. (1986) *Cell 45*, 721–732.
Joshi, S., Ogawa, H., Thompson Burke, G., Tseng, L. Y.-H., Rechler, M. M., & Katsoyannis, P. G. (1985) *Biochem. Biophys. Res. Commun. 133*, 423–429.
Klapper, D. G., Svodoba, M. E., & Van Wyk, J. J. (1983) *Endocrinology 112*, 2215–2217.
Kobayashi, M., Ohgaku, S., Iwasaki, M., Maegawa, H., Shigeta, Y., & Inouye, K. (1982) *Biochem. J. 206*, 597–603.
Misbin, R. I., & Almira, E. C. (1989) *Diabetes 38* (2), 152–158.
Misbin, R. I., Almira, E. C., & Buynitsky, S. J. (1983a) *J. Biol. Chem. 258*, 2157–2162.
Misbin, R. I., Almira, E. C., Duckworth, W. C., & Mehl, T. D. (1983b) *Endocrinology 113*, 1525.
Morgan, D. O., & Roth, R. A. (1986) *Biochemistry 25*, 1364–1371.
Muir, A., Offord, R. E., & Davies, G. J. (1986) *Biochem. J. 237*, 631–637.
Nakagawa, S. H., & Tager, H. (1987) *J. Biol. Chem. 262*, 12054–12058.
Rinderknecht, E., & Humbel, R. E. (1978a) *J. Biol. Chem. 253*, 2769–2776.
Rinderknecht, E., & Humbel, R. E. (1978b) *FEBS Lett. 89*, 283–286.
Roth, R. A., Mesirow, M. L., Yokono, K., & Baba, S. (1984) *Endocrine Res. 10* (2), 101–112.
Roth, R. A., Steele-Perkins, G., Hari, J., Stover, C., Pierce, S., Turner, J., Edman, J. C., & Rutter, W. J. (1988) *Cold Spring Harbor Symp. Quant. Biol. 53*, 537–541.
Shii, K., & Roth, R. A. (1986) *Proc. Natl. Acad. Sci. U.S.A. 83*, 4147–4151.
Shii, K., Yokono, K., Baba, S., & Roth, R. A. (1986) *Diabetes 35*, 675–683.
Stentz, F. B., Kitabchi, A. E., Schilling, J. W., Schronk, L. R., & Seyer, J. M. (1989) *J. Biol. Chem. 264*, 20275–20282.
Tager, H., Thomas, N., Assoian, R., Rubenstein, A., Saekow, M., Olefsky, J., & Kaiser, E. T. (1980) *Proc. Natl. Acad. Sci. U.S.A. 77*, 3181–3185.

Specificity and Orientation of (Iodoacetamido)proxyl Spin-Labeled Myosin Subfragment 1 Decorating Muscle Fibers: Localization of Protein-Bound Spin Labels Using SDS-PAGE†

Katalin Ajtai,‡ László Pőtő,§ and Thomas P. Burghardt*,‖
Department of Biochemistry and Molecular Biology, Mayo Foundation, Rochester, Minnesota 55905
Received January 17, 1990; Revised Manuscript Received April 12, 1990

ABSTRACT: The nitroxide spin label (iodoacetamido)proxyl (IPSL) was specifically and rigidly attached to sulfhydryl 1 (SH1) on myosin subfragment 1 (S1). The specificity of this label for SH1 was demonstrated by using a technique where the spin label is localized on the electrophoresis-isolated proteolytic fragments of myosin using electron paramagnetic resonance (EPR). Studies of the rigidity of the probe on SH1 indicate that the IPSL is immobilized on the surface of S1 in the presence and absence of the nucleotides MgADP or MgATP. The EPR spectrum of muscle fibers decorated with IPSL–S1 shows that the IPSL–S1 rotates from its orientation in rigor upon binding MgADP. The angular displacement due to nucleotide binding is larger than that detected with the (maleimido)tempo spin label [Ajtai, K., French, A. R., & Burghardt, T. P. (1989) *Biophys. J. 56*, 535–541], demonstrating that the IPSL is oriented on the myosin cross-bridge in a manner that is favorable for detecting cross-bridge rotation during the rigor to MgADP state transition.

Orientation changes of fluorescent or spin probes attached to reactive side chains on the myosin cross-bridge demonstrate the ability of the cross-bridge to maintain differing orientations while bound to the actin filament in muscle fibers. The orientation of either type of probe is characterized by a molecular coordinate frame fixed in the probe. The orientation of the probe-fixed frame can be detected (with varying degrees of angular resolution) by fluorescence polarization or electron paramagnetic resonance (EPR). For some time now we have been measuring the orientation of a variety of probes as a function of time and/or the physiological state of the muscle. We find that the probes have differing sensitivities to the cross-bridge rotation consistent with the view that some of the

† This work was supported by National Science Foundation Grant DMB-8819755 and by a grant from the Mayo Foundation.
‡ On leave from the Department of Biochemistry, Eötvös Loránd University, Budapest, Hungary.
§ On leave from the Central Laboratory of the Medical University in Pécs, Hungary.
‖ Established Investigator of the American Heart Association.

0006-2960/90/0429-7733$02.50/0

probes are oriented on the cross-bridge nearly parallel with the axis of rotation of the cross-bridge (and are rather insensitive to cross-bridge rotation) and others are more nearly perpendicular to the axis of rotation (and very sensitive to rotation).

The spin label with the maleimido reactive group, (maleimido)tempo spin label (MTSL), attached to myosin sulfhydryl 1 (SH1), rotates from its orientation in rigor upon the binding of nucleotide (Ajtai et al., 1989). This work was done by using fibers decorated with MTSL-labeled myosin subfragment 1 (S1). The orientation of the MTSL on S1 is along an axis of rotation of the S1 such that this spin label is rather insensitive to S1 rotation. This finding eliminates MTSL as a suitable probe for studying physiologically relevant cross-bridge orientation changes.

The (iodoacetamido)tempo spin label (ITSL) is oriented on the cross-bridge differently than MTSL (Thomas & Cooke, 1980). This probe can modify myosin SH1 more specifically than MTSL and was used to study cross-bridge orientation in rigor. However, it was shown that ITSL is unsuitable for studying cross-bridge orientation in any other state of the muscle since it becomes mobile when nucleotides bind to the cross-bridge (as during muscle contraction) (Seidel, 1982). We describe below an alternative spin probe that is suitable for the study of cross-bridge orientation in the nucleotide binding states of the fiber.

We find that (iodoacetamido)proxyl spin label (IPSL) is very specific for myosin SH1 due to its iodoacetamido reactive group, is immobilized on the surface of myosin in the presence and absence of nucleotides, and is oriented on the cross-bridge in a direction favorable for detecting the relevant cross-bridge orientation changes. The specificity of the IPSL for SH1 on S1 was investigated by using sodium dodecyl sulfate–polyacrylamide gel electrophoresis (SDS–PAGE) of IPSL–S1 and trypsin-digested IPSL–S1. We found that only the myosin heavy chain and its 20-kDa fragment had a nitroxide spin signal. ATPase activity measurements of IPSL–S1 confirmed that SH1 was specifically labeled with the IPSL.

Measurement of the EPR spectrum from IPSL–S1 either immobilized by precipitation of the S1 or in solution confirmed that the spin label is immobilized on SH1 in the presence and absence of nucleotides and/or that the local environment of the probe did not change significantly in these conditions. It seems likely that the planar structure of the proxyl ring (with five members rather than the six in tempo) is responsible for the stabilization of IPSL on the surface of the cross-bridge (Lajzerowicz-Bonneteau, 1976). This stability is not disturbed by cross-bridge binding of nucleotides.

Studies of the orientation of the IPSL–S1 decorating muscle fibers in rigor and in the presence of MgADP show that the IPSL–S1 rotates from its orientation in rigor when the IPSL–S1 binds MgADP. The rotation is easily detectable as a large change in the shape of the spectrum, indicating that the IPSL probe has an orientation on the S1 that is favorable for detecting S1 rotation.

Materials and Methods

Chemicals. ATP, ADP, P^1,P^5-di-5′-adenosyl pentaphosphate (Ap_5A), phenylmethanesulfonyl fluoride (PMSF), ethylenediaminetetraacetic acid (EDTA), glucose, hexokinase, creatine phosphate, creatine kinase, and bovine serum albumin (BSA) were from Sigma (St. Louis, MO). The spin label *N*-[3-(iodoacetyl)amino]-2,2,5,5-tetramethylpyrrolidine-1-oxyl [(iodoacetamido)proxyl or IPSL] was purchased from Molecular Probes (Eugene, OR). Spin labels 4-(2-iodoacetamido)-2,2,6,6-tetramethylpiperidine-1-oxyl [(iodoacetamido)tempo or ITSL], 4-isothiocyanato-2,2,6,6-tetramethylpiperidine-1-oxyl [(isothiocyanato)tempo or ITCTSL], and 4-maleimido-2,2,6,6-tetramethylpiperidine-1-oxyl [(maleimido)tempo or MTSL] were from Sigma. Ammonium sulfate (ultrapure) was from Schwartz/Mann Biotechnology (Cleveland, OH). Anion-exchange resin AG1-X8 was from Bio-Rad. All chemicals were analytical grade.

Solutions. In the fiber studies rigor solution was 80 mM potassium chloride, 5 mM magnesium chloride, 2 mM ethylene glycol bis(β-aminoethyl ether)-*N,N,N′,N′*-tetraacetic acid (EGTA), and 5 mM phosphate buffer at pH 7.0. In MgADP solution, 4 mM ADP was added to the rigor solution together with 100 μM Ap_5A to inhibit myofibrillar myokinase from converting ADP to ATP and an ADP regenerating system of 10 mM glucose and 0.1 mg/mL hexokinase to convert ATP to ADP. Relaxing solution was the same as rigor with 4 mM ATP added. Skinning solution was relaxing solution with 0.5% Triton X-100 added.

In studies with labeled S1 in solution, ATP-containing solution was the same as relaxing solution but with 10 mM ATP, 10 mM $MgCl_2$, and an ATP regenerating system consisting of 4 mM phosphocreatine and 0.3 mg/mL phosphocreatine kinase. The ADP-containing solution was the same as that used with fibers but with 10 mM ADP and 10 mM $MgCl_2$.

Preparation of Spin-Labeled Myosin Subfragment 1. Rabbit myosin was prepared by a standard method (Tonomura et al., 1966). S1 was obtained by digesting myosin filaments with α-chymotrypsin (Weeds & Taylor, 1975). S1 (30–50 μM) was labeled for 24 h with a 1.5-fold molar excess of IPSL in 50 mM TES at pH 7.0 and 4 °C. The reaction was stopped and the free label removed by the dialysis of S1 in buffer containing 25 mM potassium ferricyanide, 1 mM cysteine, 1 mM EDTA, and 50 mM TES at pH 7.0 for 12 h. This treatment selectively destroys nitroxides not linked to SH1 (Graceffa & Seidel, 1980). The potassium ferricyanide was removed in less than 2 h by adding AG1-X8 anion-exchange resin (equilibrated with 50 mM TES, pH 7.0) at 4 °C. A ratio of 0.2 g of resin/mL of solution was used for the removal of the 25 mM ferricyanide. The labeled S1 was then dialyzed in rigor buffer for the fiber decoration experiments. The treatment with ferricyanide and subsequently with the resin did not affect the ATPase activities of the control S1 or spin-labeled S1.

The labeling of S1 with MTSL or ITSL was done by a protocol identical with that described above.

Preparation of Ammonium Sulfate Precipitated Spin-Labeled S1. Dialysis bags containing spin-labeled S1 were placed in a 60% saturated ammonium sulfate solution, also containing 2 mM EDTA and 25 mM Tris-HCl at pH 8.0, and stirred overnight. The precipitated protein was collected by centrifugation. The sediment was stored at −15 °C for up to several weeks. The ammonium sulfate precipitation and subsequent storage do not alter the ATPase activity of the proteins. The precipitation of spin-labeled S1 in the presence of MgADP was done in 60% saturated ammonium sulfate, 25 mM Tris-HCl, pH 8.0, and 4 mM MgADP. It was shown that myosin precipitated with ammonium sulfate in the presence of nucleotide contains a mole to mole ratio for nucleotide to myosin of ~0.88 (Schliselfeld & Bárány, 1968).

Tryptic Digestion of S1. Labeled and unlabeled S1 was fragmented with trypsin according to Bálint et al., (1975, 1978). The digestion was carried out in 50 mM Tris-HCl at pH 8.0 and at 25 °C with a mole ratio of S1 to trypsin of 1 to 80. The proteolysis was stopped with soybean trypsin inhibitor with an inhibitor to trypsin mole ratio of 3 to 1. The

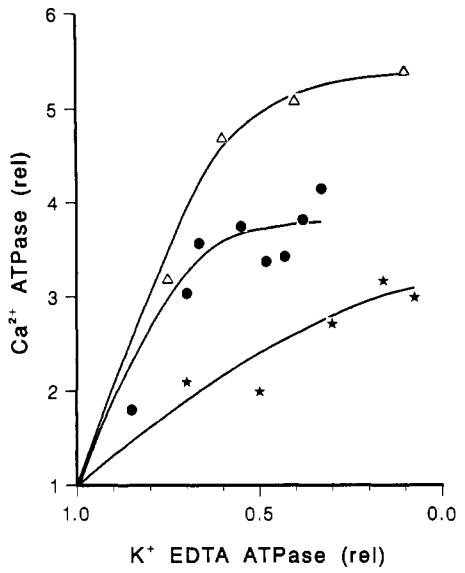

FIGURE 1: Effects of SH1 modification on the activation of Ca^{2+} ATPase in myosin S1. ITSL-modified S1 (triangles) showed the largest Ca^{2+} ATPase activation that is linear with SH1 modification until ~50% of the SH1's are modified. IPSL-S1 (closed circles) is similar to ITSL-S1. MTSL-S1 (stars) is the least linear and shows the least activation of the Ca^{2+} ATPase. These data are consistent with the view that the iodoacetamido-based probes are more specific for SH1 than MTSL and that MTSL modifies both SH1 and SH2.

samples were stored at −15 °C for up to several weeks.

Preparation of Spin-Labeled BSA. Lyophilized BSA was dissolved in 10 mM Tris-HCl, pH 8.0, at a concentration of 5 mg/mL. (Isothiocyanato)tempo was added to the BSA solution at a 10 to 1 mole ratio and allowed to react for 24 h at 4 °C. The ITCTSL reacts with the amino groups of the protein. The reaction was stopped and the free spin label was removed from the solution by gel filtration with Sephadex G-25.

Specificity of IPSL for Myosin SH1 Determined by S1 ATPase Activity. We measured the extent and specificity of the spin labeling of the SH1's using the K^+-EDTA ATPase and Ca^{2+} ATPase activities of the labeled S1 (Seidel, 1982). The Ca^{2+}- and K^+-EDTA-activated ATPase activity was measured by using the modified Fiske and SubbaRow phosphate determination method of Bârâny et al. (1967). The K^+-EDTA ATPase activity was measured in 0.6 M KCl, 6 mM EDTA, and 25 mM Tris-HCl at pH 8 and 25 °C. The Ca^{2+}-activated ATPase was measured in 0.6 M KCl, 5 mM $CaCl_2$, and 25 mM Tris-HCl at pH 8 and 30 °C. The protein concentration of the assay was 0.02–0.03 mg/mL; ATP concentration was 2.0 mM. There were nine different S1 preparations. The ATPase activities for unlabeled S1 were, for K^+-EDTA, 4.82 ± 0.02 μmol of phosphate/(mg of S1·min) and, for Ca^{2+}, 0.62 ± 0.03 μmol of phosphate/(mg of S1·min).

Shown in Figure 1 are curves representing the activation of the Ca^{2+} ATPase of labeled S1 due to the modification of SH1 with three different spin labels. The x axis represents the extent of the modification of SH1 as measured by the inhibition of the K^+-EDTA ATPase (Seidel et al., 1970; Takashi et al., 1976; Crowder & Cooke, 1984). Figure 1 shows regions of linearity where modification of SH1 is specific and regions of nonlinearity where less specific reactions occur. Modification of S1 with the iodoacetamido-based spin labels (ITSL and IPSL) causes an ATPase change characteristic of specific SH1 modification. Modification of S1 with MTSL is indicative of a less specific reaction probably involving both SH1 and SH2. We selected labeling ratios of 0.35–0.45 for IPSL, 0.3–0.5 for MTSL, and 0.5–0.7 for ITSL.

The amount of bound spin label was also measured by an independent spectroscopic method. Labeled S1 was denatured by warming to 70 °C in the presence of 1 N KOH for 1 min to mobilize the spin label on the protein. The EPR spectrum of the denatured labeled S1 was compared to identically treated solutions of spin label with known label concentrations. We observed no degradation of the spin label, in the standard spin label concentration solutions, as a result of this treatment. The result of this direct measurement of spin label stoichiometry on S1 agrees within experimental error with that obtained from the ATPase activity estimates mentioned above. The effect of ferricyanide on the protein-bound EPR signal was measured as described above. The chemical treatment eliminated 18% from the IPSL, 26% from the ITSL, and 50% from the MTSL signals.

Localization of Protein-Bound Spin Labels Using SDS–PAGE. A new method was developed to localize the spin label in the S1 using a modified SDS–PAGE protocol. IPSL-, MTSL-, and ITSL-labeled S1 were fragmented with trypsin, and the peptide composition of the digest was analyzed by SDS–PAGE (Laemmli, 1970). We optimized the electrophoresis conditions to stabilize the free radical of the spin label by leaving out oxidizing/reducing agents (such as mercaptoethanol) from the treating solutions, waiting 12 h after the polymerization of the running gel before using it with spin-labeled proteins to deplete the gel of the polymerization products (such as TEMED and ammonium persulfate) that react with free spins, and washing the slab gel prepared for the electrophoresis by prerunning it with buffer. A Bio-Rad mini protean cell was used with a preparative comb to minimize the running time and to get a homogeneous peptide band that fits in the EPR tissue sample cell.

After completion of the electrophoresis the regions of the slab gel corresponding to the peptides of interest were selected by comparison of a Commassie-stained and unstained section of the same gel. To detect the peptide-bound spin labels, the unstained gel bands were subsequently washed with a solution of 10% ethanol and dried, with circulating room temperature air, between two cellophane sheets. Dried samples containing 30–200 μg of protein were placed in the EPR spectrometer to detect the spin. Depending on the intensity of the EPR signal, 30 min–2 h data collection times were required.

All of the gel manipulations were done in the dark to avoid photodegradation of the spin label. The dried gel samples could be stored in the dark at room temperature for months without any loss of EPR signal intensity.

Preparation of Muscle Fibers. Rabbit psoas muscle fibers were obtained as previously described (Borejdo et al., 1979) and kept in a relaxing solution containing 50% glycerol (volume to volume) at −15 °C for up to several weeks. Before decoration with S1, bundles of ~50 glycerinated fibers each were washed for 30 min in relaxing solution, to remove the glycerol, and then transferred to skinning solution for 30 min, to remove cell membranes that may inhibit diffusion of S1 through the fiber bundles. The fibers were then thoroughly washed first in relaxing solution (15 min) and then in rigor solution (20 min). These fiber bundles were incubated in rigor buffer containing spin-labeled S1 at a concentration of 4–6 mg/mL for 6–24 h in the dark at 4 °C. PMSF was added at 100 μM concentration to the rigor solution during incubation of the fibers with spin-labeled S1 to inhibit tissue proteases from digesting the fiber. The labeled fiber bundles were washed in rigor for ~30 min to remove the unbound S1 and then incubated in either rigor or ADP solution for 30 min. The

fibers were then cut to a uniform length of ~4 mm and arranged with parallel fiber axes in a quartz flat tissue cell (Wilmad Glass, Buena, NJ) for the EPR studies.

The manipulations of the fibers before placing them in the flat cell were done at 4 °C. Once in the flat cell the fibers were allowed to warm up to room temperature and the EPR spectra were measured at room temperature.

We estimated the contribution of free IPSL–S1 to the decorated fiber spectrum by comparing the fiber spectrum (in both the presence and absence of MgADP) to that obtained from IPSL–S1 in solution. The free IPSL–S1 in rigor and in the presence of MgADP had identical spectra that were characteristic of a randomly oriented, slowly moving, spin label. The decorated fiber spectrum at zero tilt relative to the Zeeman field showed no trace of the low-field resonance characteristic of free IPSL–S1.

EPR Measurements of the Effect of Nucleotides on Spin-Labeled S1 in Solution. All EPR measurements were carried out on a Bruker Model ER200 series instrument using a TM_{110} cylindrical cavity. All spectra were recorded at 10-mW microwave power and with a modulation amplitude of 1.0–3.0 G.

The free protein solutions were measured in standard 0.3-mm aqueous EPR flat cells. Labeled S1 (4–8 mg/mL) was used in all of the free protein experiments. The ATP-containing solution was prepared at 0 °C and immediately loaded into an EPR cuvette. Once in the cuvette the solution was allowed to warm up to room temperature and the spectra were measured. The EPR measurements in the presence of ATP were conducted within 3–11 min after the mixing of the labeled S1 with the ATP. We used the effect of bound nucleotide on the mobility of ITSL labeling S1 to ascertain that during this time period the ATP regenerating system held the ATP concentration constant. We observed, during the first 2–3 min after the mixing of ITSL–S1 and ATP, an incomplete ATP effect such that the spectral line shape was between that observed for rigor and that in the presence of ATP after 3 min. From 3 to 11 min after mixing we observed a steady-state line shape that was typical of the ATP effect. At later times the spectra approached those characteristic of ITSL–S1 in the presence of ADP.

EPR Measurements on Decorated Fibers. The TM_{110} cavity has zero electric field along a plane containing the Zeeman magnetic field and the axis along which the sample is inserted into the cavity (the sample axis). Two spectra were measured from each fiber sample such that one spectrum (zero tilt) originated from fibers whose fiber axis was parallel to the Zeeman field and the second spectrum from fibers at 90° to the zero tilt spectrum. The zero tilt spectrum is measured when the flat cell is in the zero electric field plane. Tilted spectra were measured by rotating the flat cell about the sample axis and relative to the Zeeman field. This procedure produces the tilt series of EPR spectra needed in our analysis (Burghardt & French, 1989). The measurement of both spectra in a tilt series was completed in approximately 30 min.

The derivatives of the EPR absorption spectra were digitized into 4096 data points at equal intervals over the sweep width of the Zeeman field and temporarily stored on a floppy disk. Later the spectra were transferred to the disk of a larger computer for analysis. The EPR spectra were subjected to a linear baseline correction to set the low- and high-field asymptotic absorption, and total area under the curve, equal to zero. Spectra were normalized arbitrarily.

Numerical Analysis of EPR Spectra. Sets of up to 21 tilt series spectra were simultaneously analyzed by the method described and used previously (Burghardt & French, 1989; Ajtai et al., 1989), to derive the order parameters of the probe angular distribution. In this method spectral parameters, such as the values of the elements of the g and T tensors, are varied to minimize a fitting quality factor, Q, defined in eq 20 of Burghardt and French (1989). The probe angular distribution is reconstructed by using the relation:

$$N(\Omega) = \sum_{j=0}^{j_{max}} \sum_{m,n=-j}^{j} a^j_{m,n} \left(\frac{2j+1}{8\pi^2} \right)^{1/2} D^j_{m,n}(\Omega) \qquad (1)$$

where $\Omega = (\alpha, \beta, \gamma)$ are the Euler angles of the probe orientation, $a^j_{m,n}$ is the order parameter, $D^j_{m,n}$ is a Wigner function (Davydov, 1963), and j_{max} is the maximum rank of the measured order parameters. We also use the polar angular distribution, $n(\beta)$, derived from eq 1, by averaging over α and γ such that

$$n(\beta) = \sum_{j=0}^{j_{max}} a^j_{0,0} \left(\frac{2j+1}{8\pi^2} \right)^{1/2} P_j(\cos \beta) \qquad (2)$$

where $P_j(\cos \beta)$ is a Legendre polynomial (Arfken, 1970).

The computer program implementing the analysis formalism is written in FORTRAN. The simultaneous analysis of 21 tilt series data sets consisting of 42 EPR spectra could typically be completed within ~12 h of CPU time on a VAX 8810.

Results

Evidence for the Specific Labeling of SH1 by IPSL. The EPR detection of protein-bound spin labels was carried out on different proteins (myosin S1 and its proteolytic fragments or BSA) labeled with various nitroxide spin labels (IPSL, MTSL, ITSL, and ITCTSL). Shown in Figure 2 are the EPR spectra from the dried slab gels. Figure 2A shows a Coomassie-stained SDS–PAGE electrophoretogram of (isothiocyanato)tempo-labeled BSA and two corresponding EPR spectra measured from the dried gel. The background signals are measured from protein-free sections of the same gel and indicate the typical noise from the spectrometer with this gel preparation. This EPR signal is from 130 μg of the ITCSL–BSA. Figure 2B shows the Coomassie-stained SDS–PAGE electrophoretogram of spin-labeled S1 together with the corresponding EPR spectra. The left (right) side shows the results from proteins before (after) treatment with ferricyanide. Shown in Figure 2C are EPR spectra from dried gels containing the proteolytic fragments of spin labeled S1. The left (right) side shows the results from peptides derived from spin-labeled S1 before (after) treatment with ferricyanide.

The degree of specificity of the spin labeling of the S1 is indicated by the intensity of the EPR spectra measured from the protein or protein fragment isolated in the gel. Figure 2B shows that, in spin-labeled S1, the dominant EPR signal was found in the heavy chain of the S1 with some labeling of LC_1 in the case of MTSL. This side label was eliminated by treating the protein with ferricyanide (compare the left and right panels of Figure 2B). The comparison of the intensities of the EPR spectra from ferricyanide-treated, spin-labeled S1 indicates that ≥95% of the spin signal originates from the heavy chain of S1.

Figure 2C shows that for each spin probe the dominant EPR signal was found in the 20-kDa fragment. In the case of MTSL–S1 before treatment with ferricyanide some bound spin label was found on the 27-kDa fragment, suggesting that MTSL reacts with the reactive lysyl groups of S1. The comparison of the intensities of the EPR spectra from the ferricyanide-treated and digested, spin-labeled S1 indicates that

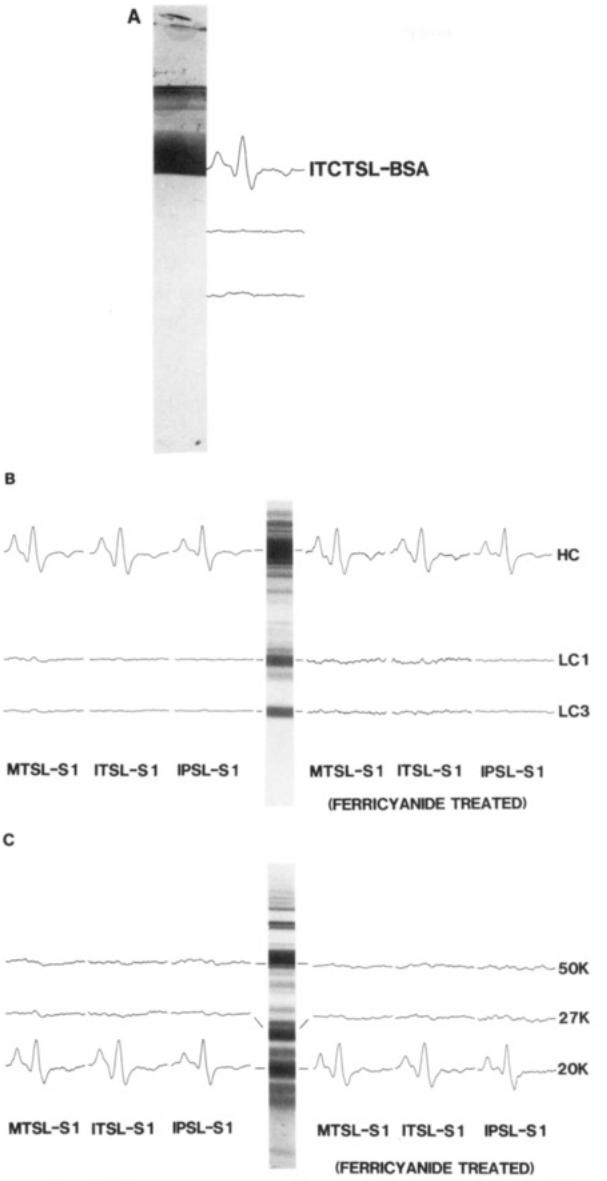

FIGURE 2: EPR measurement of protein-bound spin label from SDS–PAGE electrophoretogram. Panel A indicates the EPR signals from the gel bands containing ITCSL–BSA and two others containing no protein. Panel B indicates the EPR signal from gel bands containing MTSL, ITSL, and IPSL–S1 showing the spin label localization in either the myosin heavy chain (HC) or the light chains (LC) 1 and 3, before (left) and after (right) treatment with ferricyanide. Panel C indicates the EPR signals from gel bands containing the tryptic digest of MTSL, ITSL, and IPSL–S1 showing the spin label localization in the proteolytic fragments of S1 before (left) and after (right) treatment with ferricyanide. The spectral intensities show that, for every spin probe, after treatment with ferricyanide, ≥95% of the spin intensity was contained in the myosin heavy chain and in the 20-kDa fragment. Before treatment with ferricyanide, the MTSL–S1 exhibited a small spin signal from LC1 and the 27-kDa fragment.

≥95% of the spin signal originates from the 20-kDa fragment of S1 containing the reactive thiols SH1 and SH2. From the four cysteines of the 20-kDa fragment (Hozumi, 1982) only two react with SH reagents in the native structure of S1 (Schaub et al., 1975; Takashi et al., 1976; Balint et al., 1978). These findings, together with the results of our ATPase results (see Materials and Methods), show conclusively that ferricyanide-treated IPSL–S1 is specifically labeled at SH1.

The sensitivity of the method for detecting a spin label seems comparable to that achievable with optical scanning of gels containing proteins labeled with fluorescent probes. The signal-to-noise ratio of our measurements allowed us to detect a spin signal from ~5% of the total detected intensity.

Rigidity of the IPSL on SH1. The EPR spectra from IPSL–S1, MTSL–S1, and ITSL–S1 in solution and after precipitation with ammonium sulfate were recorded before and after treatment with ferricyanide. Before treatment with ferricyanide, spectra from spin-labeled S1 in solution are a superposition of spectra from slowly and rapidly moving probes. After treatment with ferricyanide, spectra from labeled S1 in solution and in the absence of nucleotide retained only the spectral component of the slowly moving probes. The slowly moving probe spectrum is characteristic of a spin probe undergoing rotational Brownian motion due to the slow rotational diffusion of the S1 molecule. These findings indicate that the ferricyanide treatment selectively destroyed the spin of the independently mobile, nonspecific spin label, for each of the spin labels.

Figure 3 shows EPR spectra of spin-labeled S1 in solution after treatment with ferricyanide, and in the presence or absence of nucleotides. Spectra are averages of five to eight measurements from independently prepared samples. Panel A shows the spectra from IPSL–S1. Spectra measured from IPSL–S1 in the absence of nucleotides, in the presence of MgADP, and in the presence of MgATP are identical to within experimental error, indicating no measurable effect of nucleotide binding on the mobility or environment of IPSL on SH1. Panel B shows the effect of nucleotide binding to S1 on the mobility of ITSL/S1. As observed previously (Seidel et al., 1970; Seidel & Gergely, 1973; Wells & Bagshaw, 1984), the binding of MgADP or MgATP affects probe mobility such that the probe is more mobile in the presence of these nucleotides. Panel C shows the effect of nucleotide binding to S1 on the mobility of MTSL–S1. As is the case with IPSL–S1 and as observed previously (Seidel, 1982; Thomas et al., 1980; Wells & Bagshaw, 1984), the binding of MgADP or MgATP has no effect on probe environment or mobility.

Figure 4 shows EPR spectra from ammonium sulfate precipitated, spin-labeled S1 before and after treatment with ferricyanide. Comparison of panel C (MTSL–S1) with panels A and B (IPSL–S1 and ITSL–S1) indicates that treatment with ferricyanide removes a larger fraction of nonspecific label from MTSL–S1 (~50%) compared to the iodoacetamido-based spin labels since the MTSL–S1 spectra undergo a larger change due to this treatment.

The comparison of spectra from ferricyanide-treated spin-labeled S1, precipitated or freely moving in solution, should allow us to estimate the relaxation time of the probe motion provided we can assume that the spectra from the precipitated protein is that of an immobilized spin probe. This relaxation time would reflect the combination of motions due to protein rotation and the independent rotational motion of the probe. Freed (1976) described a model calculation of this type where the separation of the hyperfine extrema of the EPR spectrum from probes rotating in solution can be compared with this splitting from immobilized probes, to estimate the probe rotational relaxation time in solution. The model calculation shows that a decreasing separation between the hyperfine extrema indicates an increase in probe mobility.

Our results for IPSL-, ITSL-, and MTSL-labeled S1 are summarized in Table I. As expected, probes are more mobile in solution than in the precipitated form. This mobilization is constant in the presence and absence of nucleotides, to within the experimental error, for MTSL–S1 and IPSL–S1. As observed previously (Seidel & Gergely, 1973; Wells & Bagshaw, 1984), the mobility of ITSL–S1 is dependent on the occupancy of the nucleotide binding site.

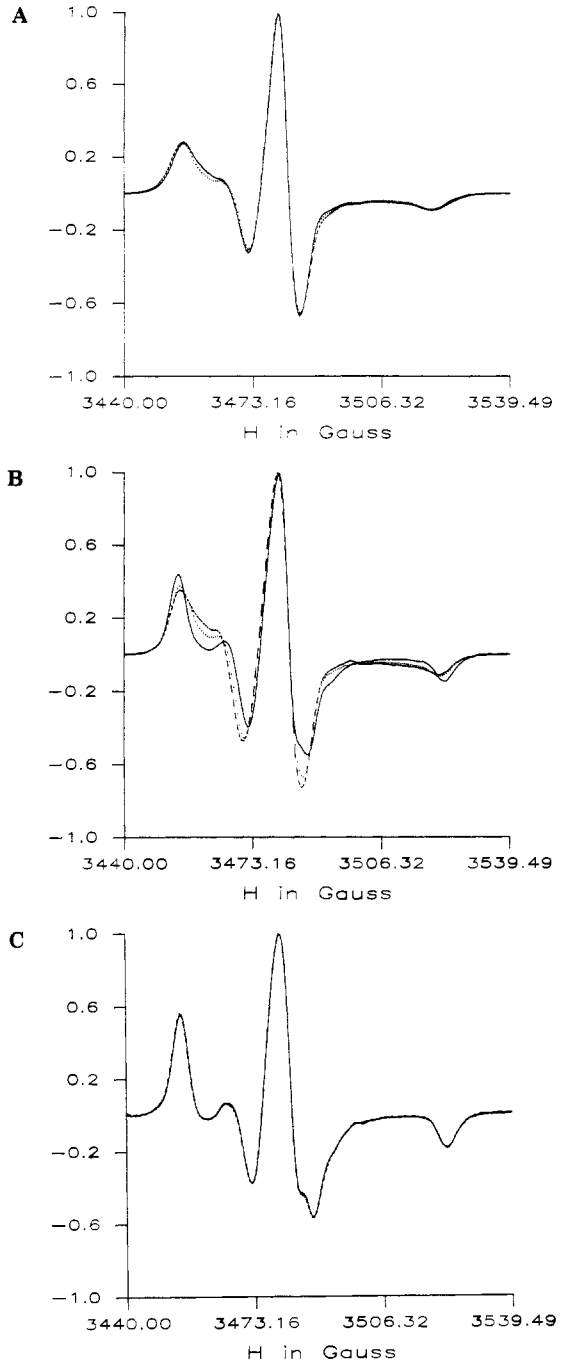

FIGURE 3: EPR spectra from IPSL–S1 (A), ITSL–S1 (B), and MTSL–S1 (C) in rigor buffer (lines), in the presence of MgATP (dots), and in the presence of MgADP (dashes). The spectra are averages of five to eight measurements of independently prepared samples. In panel A the spectra from IPSL–S1 are identical to within experimental error, indicating no change in the environment or mobility of the IPSL in these conditions. In panel B the spectra from ITSL–S1 indicate the presence of nucleotide causes a mobilization of the probe. In panel C the spectra from MTSL–S1 are identical to within experimental error, indicating no change in the environment or mobility of the MTSL in these conditions.

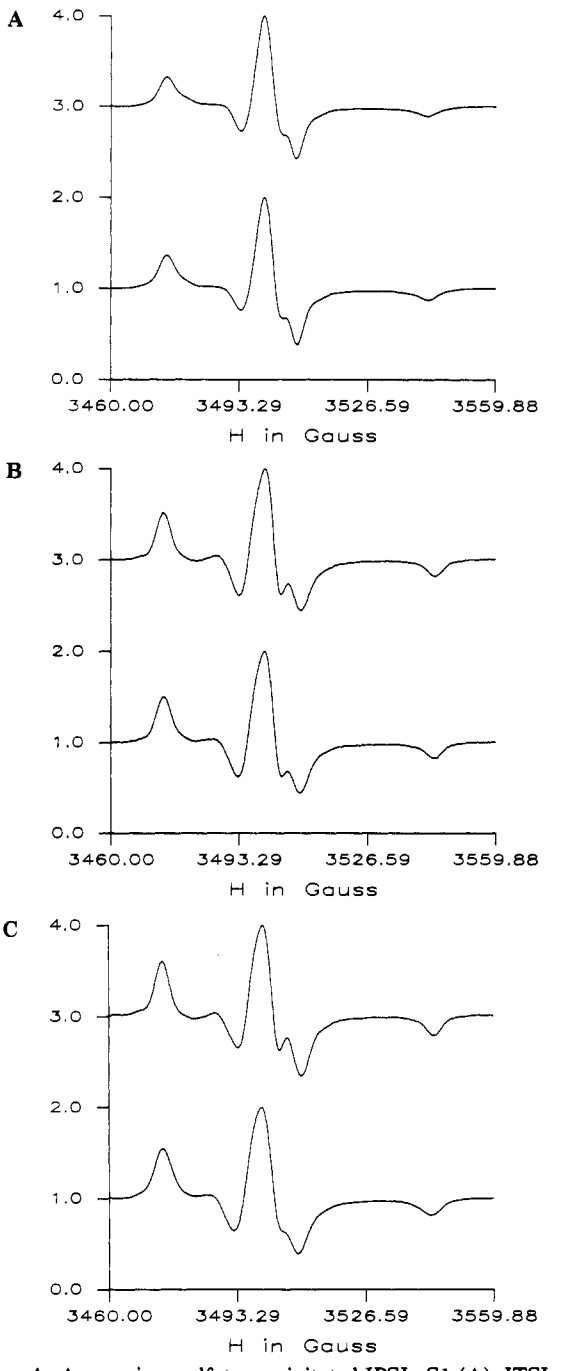

FIGURE 4: Ammonium sulfate precipitated IPSL–S1 (A), ITSL–S1 (B), and MTSL–S1 (C) before (top) and after (bottom) treatment with ferricyanide. Spectra from MTSL–S1 show a clear difference due to the treatment with ferricyanide, indicating a large fraction of nonspecific probe is eliminated by the treatment.

The effect of MgADP binding to IPSL–S1 was also investigated by using the precipitated form of IPSL–S1. We measured the hyperfine extrema of IPSL–S1 precipitated from rigor and in the presence of MgADP. These measurements, also shown in Table I, suggest that the local environment of the probe *is unperturbed* by the binding of MgADP to IPSL-S1.

EPR Spectroscopy from IPSL–S1 Decorating Fibers. The tilt series EPR spectra from fibers decorated with IPSL–S1, in rigor and in the presence of MgADP, are shown in Figure 5. As shown, the tilt series consists of two spectra, one from a decorated fiber oriented with its fiber axis parallel to the Zeeman field and the other orthogonal to this direction. The spectra shown are averages of 42 spectral measurements, 24 from fibers in rigor and 18 from fibers in the presence of MgADP.

From the tilt series data sets shown in Figure 5, plus four independent tilt series data sets each consisting of 42 spectra, we ascertained the spectral parameters for decorated fibers in rigor and in the presence of MgADP. We found that the spectral parameters for these two fiber states are identical and are given by $g_x = 2.0085 \pm 0.0005$, $g_y = 2.0055 \pm 0.0005$, $g_z = 2.0020 \pm 0.0005$, $T_x = 6.5 \pm 0.5$ G, $T_y = 5.0 \pm 0.5$ G, and

Table I: Hyperfine Extrema from Spin-Labeled Myosin S1[a]

probe	condition	precipitated S1	solution S1
IPSL	rigor	67.65 ± 0.1	63.84 ± 0.2
	MgATP		64.27 ± 0.2
	MgADP	67.75 ± 0.1	64.10 ± 0.2
ITSL	rigor	70.5 ± 0.1	68.77 ± 0.2
	MgATP		66.55 ± 0.2
	MgADP		66.95 ± 0.2
MTSL	rigor	70.6 ± 0.1	68.50 ± 0.1
	MgATP		68.76 ± 0.1
	MgADP		68.61 ± 0.1

[a] Numbers indicate separation in gauss. Uncertainties indicate standard error of the mean. Nine different S1 preparations were used to measure these extrema.

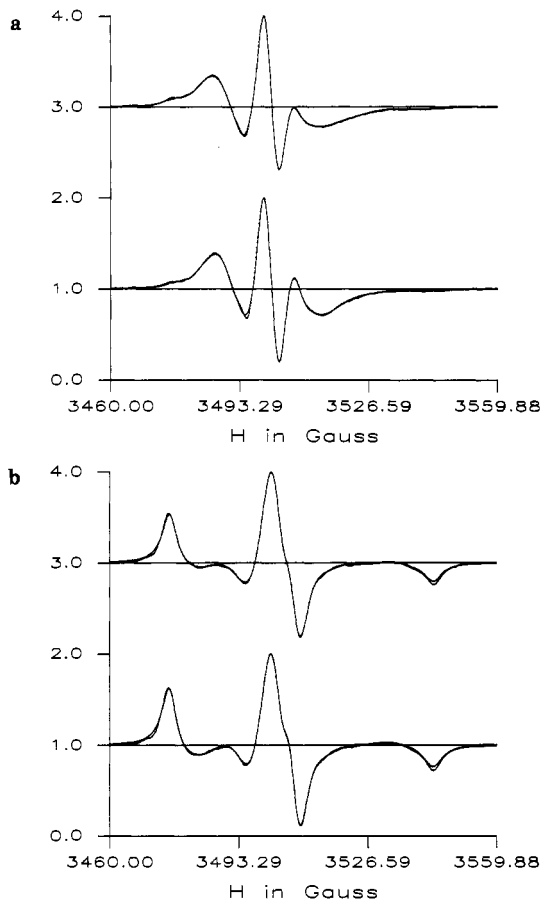

FIGURE 5: Averaged tilt series EPR spectra for fibers decorated with spin-labeled S1 in rigor and in the presence of MgADP. Panels a and b contain rigor (bottom) and MgADP (top) spectra with tilt angles $\Psi = 0°$ and 90°. Dots correspond to the data, and the solid line is the best fit as judged by minimizing the fitting quality factor, Q [see eq 20, Burghardt and French (1989)]. The maximum heights of the spectra are normalized to 1.

$T_z = 34.0 \pm 0.5$ G, where g_i are elements of the g tensor coupling the electron spin of the nitroxide to the Zeeman field and T_i are elements of the T tensor coupling the electron spin to the nuclear spin of the nitrogen in the nitroxide.

The probe angular distribution of the zero tilt fibers is assumed not to depend on the Euler angle α. The angle α corresponds to the azimuthal angle of the probe when the z axis points along the fiber axis. The fiber axis is generally assumed to be a symmetry axis of the fiber, and experimental evidence supports this assumption (Burghardt et al., 1983). This implies that for the zero tilt spectrum

$$a^j_{m,n} = a^j_{0,n}\delta_{m,0} \quad (3)$$

where $\delta_{i,j}$ is the Kronecker δ. It is reasonable to align the fiber axis with the Zeeman field for the zero tilt spectrum since the EPR signal is insensitive to probe distributions in α (Burghardt & Thompson, 1985). Thus, if eq 3 is valid, there is no loss of information from the insensitivity of the EPR signal to α.

Table II: Order Parameters from IPSL–S1 Decorated Muscle Fiber[a]

$a^j_{m,n}$	rigor	SEM	MgADP	SEM
$a^0_{0,0}$	0.1125	0.0	0.1125	0.0
$a^2_{0,0}$	−0.077	0.001	−0.069	0.002
$a^2_{0,2} + a^2_{0,-2}$	0.067	0.002	0.076	0.006
$a^4_{0,0}$	0.029	0.002	0.018	0.002
$a^4_{0,2} + a^4_{0,-2}$	−0.031	0.002	−0.020	0.002
$a^4_{0,4} + a^4_{0,-4}$	−0.22	0.02	−0.25	0.03
$a^6_{0,0}$	0.0070	0.0008	0.015	0.002
$a^6_{0,2} + a^6_{0,-2}$	0.000	0.001	0.016	0.003
$a^6_{0,4} + a^6_{0,-4}$	0.04	0.04	−0.10	0.007
$a^8_{0,0}$	−0.031	0.001	−0.033	0.002
$a^8_{0,2} + a^8_{0,-2}$	0.017	0.002	0.034	0.006
$a^8_{0,4} + a^8_{0,-4}$	0.07	0.03	−0.08	0.06
$a^{10}_{0,0}$	0.035	0.002	0.029	0.001
$a^{10}_{0,2} + a^{10}_{0,-2}$	−0.034	0.005	−0.035	0.002
$a^{10}_{0,4} + a^{10}_{0,-4}$	0.11	0.02	0.00	0.04
$a^{12}_{0,0}$	−0.025	0.002	−0.016	0.001
$a^{12}_{0,2} + a^{12}_{0,-2}$	0.030	0.001	0.029	0.003
$a^{12}_{0,4} + a^{12}_{0,-4}$	0.13	0.01	0.08	0.02
$a^{14}_{0,0}$	0.016	0.001	0.004	0.001
$a^{14}_{0,2} + a^{14}_{0,-2}$	−0.017	0.005	−0.032	0.003
$a^{14}_{0,4} + a^{14}_{0,-4}$	0.041	0.008	0.00	0.01
$a^{16}_{0,0}$	−0.005	0.002	0.007	0.002
$a^{16}_{0,2} + a^{16}_{0,-2}$	0.012	0.001	0.001	0.003
$a^{16}_{0,4} + a^{16}_{0,-4}$	0.075	0.007	0.089	0.005

[a] Order parameters deduced from tilt series EPR spectra of muscle fibers decorated with IPSL–S1 in rigor and in the presence of MgADP. The standard error of the mean (SEM) is calculated from 24 or 18 independent measurements of decorated fibers in rigor or in the presence of MgADP. The order parameters pertain to the fiber distribution at zero tilt to the Zeeman magnetic field.

The order parameters and their standard error in the mean (SEM), derived from the tilt series data sets by a model-independent method described elsewhere (Burghardt & French, 1989), are summarized in Table II, where only the order parameters from the zero tilt spectra are listed. These values indicate that there are significant differences in the probe angular distribution between the two states. The three-dimensional representation of the probe angular distribution, N from eq 1, is shown in Figure 6. The Euler angles β and γ, where β corresponds to the polar angle measured relative to the fiber axis and γ to the torsional angle, are plotted on the x and y axes while the height of the distribution is plotted on the z axis. Angles β and γ define the orientation of the principal magnetic frame of the spin label where the g and T tensors are diagonal. The plots are generated by using eqs 1 and 3. Only a finite number of the order parameters are practically calculable so that the sum in eq 1 is truncated at $j_{max} = 16$. We choose $j_{max} = 16$ since it is the maximum rank of the order parameter that is significant given the signal-to-noise ratio of our experimental data. The surfaces in Figure 6 are rippled due to the limitation on the angular resolution by the condition that $j \leq j_{max}$.

The plots in Figure 6 show that the binding of MgADP to the S1 causes a rotation that shifts the spin density to lower values of the polar angle β, while the γ degree of freedom is practically unchanged. The change in the probe distribution in the β degree of freedom is more clearly indicated in Figure 7. There the polar angular distributions, derived by averaging the angular distributions in Figure 6 over γ (see eq 2), show

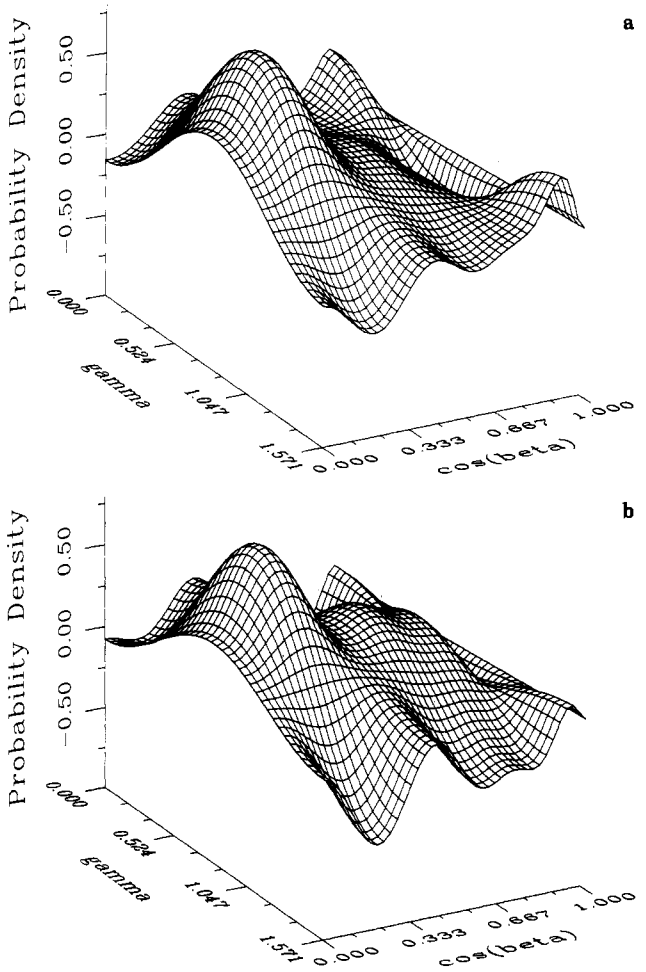

FIGURE 6: Spin probe angular distributions, N, computed from the average order parameters listed in Table II from muscle fibers decorated with spin-labeled S1 in rigor (a) and in the presence of MgADP (b). N is computed from eq 1 in the text.

the polar angle shift in the orientation of IPSL–S1 caused by the binding of MgADP to S1. Figure 7 suggests that the probe rotates in its polar angle ≥3° from its rigor orientation upon the binding of MgADP. This magnitude of angular displacement is easily resolved from the changes in the EPR spectrum apparent in Figure 5.

Discussion

Recently we showed that MTSL-labeled S1, decorating muscle fibers, rotates from its rigor orientation upon the binding of MgADP to S1 (Ajtai et al., 1989). The effect of S1 rotation is observed with the MTSL spin label as a change in the torsion angle γ. The effect of a change in γ, on the EPR spectrum from MTSL–S1 decorated fibers, is subtle and gave rise to conflicting reports about the effect of MgADP on cross-bridge orientation. Here, we show that the IPSL probe is more sensitive to the S1 rotation induced by MgADP. This is due to the favorable orientation of the IPSL relative to S1 when modifying SH1.

These results agree with our previous work using fluorescent probes. We showed earlier that S1, when modified with the fluorescent probes (iodoacetamido)tetramethylrhodamine (IATR) and 1,5-IAEDANS, rotated upon binding MgADP (Burghardt et al., 1983; Ajtai & Burghardt, 1987). The IATR probe was very sensitive to this rotation while the 1,5-IAEDANS was rather insensitive. We suggested that this difference in sensitivities was due to the differing orientations of the probes on the cross-bridge such that the transition dipole

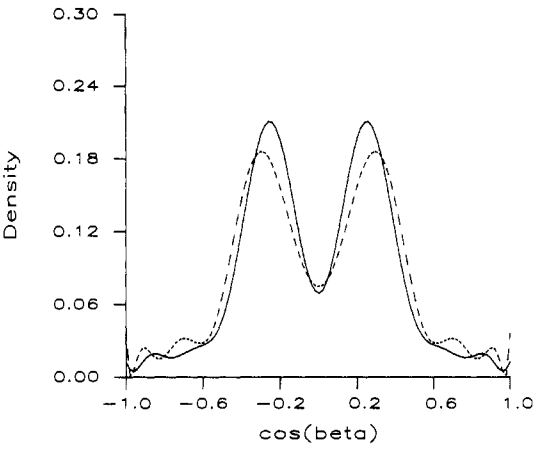

FIGURE 7: Polar probe angular distribution, $n(\beta)$, computed from order parameters in Table II from fibers decorated with spin-labeled S1 in rigor (—) and in the presence of MgADP (- - -). n is computed from eq 2 in the text.

of IATR was in a favorable, while the dipole of 1,5-IAEDANS was in an unfavorable, orientation for detecting cross-bridge rotation. This explanation was confirmed by using the technique of wavelength-dependent fluorescence polarization where the transition dipole orientation of the 1,5-IAEDANS was changed, by varying the wavelength of the excitation light, and the cross-bridge rotation caused by the binding of MgADP was detected. An EPR technique, analogous to wavelength-dependent fluorescence polarization, does not presently exist so that only by finding a probe oriented more favorably than MTSL were we able to more easily detect S1 rotation.

In our effort to find a more appropriate spin probe to detect cross-bridge rotation we developed a new method for determining the specificity of spin labels. The problem of localizing spin labels on the side chains of myosin is complicated by the use of ferricyanide to selectively destroy radicals not on SH1. The treatment with ferricyanide separates the spin probes into populations with and without a measurable EPR signal. A common method to identify a label in a peptide derived from a larger protein uses a radioisotope form of the label that can be traced by its radio emissions. The isotope does not distinguish between the spin probe populations with and without a measurable EPR signal. The use of other biochemical and organic chemical methods for determining probe specificity is questionable because of the instability of the free radical in the spin probe. We developed a method of spin probe localization that is similar to that used for fluorescent probes with some modifications employed to protect the spin label from degradation during the separation of the proteolytic fragments of myosin.

The localization of fluorescent probes in the peptides resulting from the digestion of S1 is routine because the fluorescent probes are resistant to degradation in the SDS–PAGE peptide separation process. Consequently, with fluorescent probes the specificity of new labels is determined by optically detecting the fluorescent peptide bands on the gel and comparing the pattern to a Coomassie-stained digestion pattern. Nitroxide radicals are degraded by the usual SDS–PAGE separation process, but we developed a protocol to preserve the spin while separating the peptides. The spin labels in the gel are detected by using EPR. Our method allows the spin label specificity to be determined directly from the gel as it is done with fluorescent probes.

Our new method of determining spin label location on peptides indicates that the iodoacetamido-based spin labels (ITSL and IPSL) reacted with the same selectivity for the

fast-reacting SH's on the heavy chain of S1. We detected the maleimido-based probe (MTSL) on at least two other points in S1, LC1 and the 27-kDa fragment of the heavy chain. We were also able to show that treatment with ferricyanide destroyed the EPR signals from these nonspecific probes. This method of the EPR detection of spin labels in gels is a generally useful technique for determining the specificity of protein-bound spin labels. Our discovery of a spin label that detects cross-bridge rotation as a change in the probe's polar angle β makes practical (from an EPR spectroscopist's point of view) a detailed experimental study of cross-bridge orientation as a function of the physiological or mechanical state of the fiber (Burghardt & Ajtai, 1989). Biochemically, the generalization of a specific labeling protocol from isolated S1 to glycerinated muscle fibers is not always straightforward. We are presently working out this protocol. Our newly developed tools for determining probe specificity described above, and our analytical methods for determining the probe angular distribution from the shape of the EPR spectrum that were recently described elsewhere (Burghardt & French, 1989), will be helpful in the future studies of muscle contraction using IPSL.

Acknowledgments

We thank Dr. Chris Haydock of the Mayo Foundation for assistance with the plotting software and Heidi Evans for excellent technical assistance. Computer time was furnished by the Research Computer Facility of the Mayo Foundation.

Registry No. MgADP, 7384-99-8; IPSL, 27048-01-7; ITSL, 25713-24-0; MTSL, 15178-63-9; potassium ferricyanide, 13746-66-2.

References

Ajtai, K., & Burghardt, T. P. (1987) *Biochemistry 26*, 4517–4523.

Ajtai, K., French, A. R., & Burghardt, T. P. (1989) *Biophys. J. 56*, 535–541.

Arfken, G. (1970) *Mathematical Methods for Physicists*, pp 534–608, Academic Press, New York.

Bâlint, M., Srêter, F., Wolf, I., Nagy, B., & Gergely, J. (1975) *J. Biol. Chem. 250*, 6177–6188.

Bâlint, M., Wolf, I., Tarcsafalvi, J., Gergely, J., & Srêter, F. (1978) *Arch. Biochem. Biophys. 190*, 793–799.

Bârány, M., Conover, T. E., Schliselfeld, L. H., Gaetjens, E., & Goffart, M. (1967) *Eur. J. Biochem. 2*, 156–164.

Borejdo, J., Putnam, S., & Morales, M. F. (1979) *Proc. Natl. Acad. Sci. U.S.A. 76*, 6346–6350.

Burghardt, T. P., & Thompson, N. L. (1985) *Biophys. J. 48*, 401–409.

Burghardt, T. P., & Ajtai, K. (1989) *Proc. Natl. Acad. Sci. U.S.A. 86*, 5366–5370.

Burghardt, T. P., & French, A. R. (1989) *Biophys. J. 56*, 525–534.

Burghardt, T. P., Ando, T., & Borejdo, J. (1983) *Proc. Natl. Acad. Sci. U.S.A. 80*, 7515–7519.

Crowder, M. S., & Cooke, R. (1984) *J. Muscle Res. Cell Motil. 5*, 131–146.

Davydov, A. S. (1963) *Quantum Mechanics*, pp 153–170, N.E.O. Press, Ann Arbor, MI.

Freed, J. H. (1976) in *Spin Labeling: Theory and Application* (Berliner, L. J., Ed.) Vol. 1, pp 53–132, Academic Press, New York.

Graceffa, P., & Seidel, J. C. (1980) *Biochemistry 19*, 33–39.

Hozumi, T. (1982) *J. Biochem. 91*, 1817–1819.

Laemmli, U. K. (1970) *Nature (London) 227*, 680–685.

Lajzerowicz-Bonneteau, J. (1976) in *Spin Labeling: Theory and Applications* (Berliner, L. J., Ed.) Vol. 1, pp 239–246, Academic Press, New York.

Schaub, M. C., Watterson, J. G., & Waser, P. G. (1975) *Hoppe-Seyler's Z. Physiol. Chem. 356*, 325–339.

Schliselfeld, L. H., & Bârány, M. (1968) *Biochemistry 7*, 3206–3213.

Seidel, J. C. (1982) *Methods Enzymol. 85*, 594–624.

Seidel, J. C., & Gergely, J. (1973) *Arch. Biochem. 158*, 853–863.

Seidel, J. C., Chopek, M., & Gergely, J. (1970) *Biochemistry 9*, 3265–3272.

Takashi, R., Duke, J., Ue, K., & Morales, M. F. (1976) *Arch. Biochem. Biophys. 175*, 279–283.

Thomas, D. D., & Cooke, R. (1980) *Biophys. J. 32*, 891–906.

Thomas, D. D., Ishiwata, S., Seidel, J. C., & Gergely, J. (1980) *Biophys. J. 32*, 873–887.

Tonomura, Y., Appel, P., & Morales, M. F. (1966) *Biochemistry 5*, 515–521.

Weeds, A. G., & Taylor, R. S. (1975) *Nature (London) 257*, 54–56.

Wells, C., & Bagshaw, C. R. (1984) *J. Muscle Res. Cell Motil. 5*, 97–112.